# From Empiricism, Through Theory, To Problem Solving in Rock Engineering:

# a shortened version of the 6th Müller Lecture

Nick Barton
*NB&A, Oslo, Norway.*

**ABSTRACT:** The behaviour of the jointed-and-faulted-anisotropic-water-bearing media that we call rock masses, was an abiding pre-occupation of Leopold Müller. The author has been similarly pre-occupied. So starting with modest developments from tension-fractured physical models, and progressing to the real jointed and three-dimensional world in due course, a few of the numerous lessons learned and subsequently applied in rock engineering practice will be described. These included non-linear and block-size dependent shear strength, no actual cohesion, and the possibility of thermal over-closure if rock joints are rough. A six orders of magnitude rock quality Q-scale has proved essential. Discontinuous behaviour provides rich experiences for those who value reality, even when reality has to be simplified by some empiricism.

**KEYWORDS:** rock joints, rock masses, physical modelling, empiricism, site characterization, tunnelling, rock failure

## 1. INTRODUCTION

*Figure 1. Confronted with this potentially unstable jointed rock slope, multiple reasons for the over-break and instability suggest themselves. There are clearly adverse values of JRC, JCS, and $\phi_r$, and there are also adverse ratings of Jn, Jr, Ja (and Jw on occasion).*

The lessons learned during the development of these empirical parameters, which are now widely used in many countries, will be summarised in the following pages. Their application has been in widely diverse projects.

## 2. TWO-DIMENSIONAL ROCK MASSES SIMULATED WITH PHYSICAL AND NUMERICAL MODELS

The desire to model the behaviour of jointed rock slopes in late nineteen sixties Ph.D. studies at Imperial College, led to tension-fracture models by the writer, and numerical modelling developments (pre-μDEC) in the case of student colleague Peter Cundall. The relative *inflexibility* and

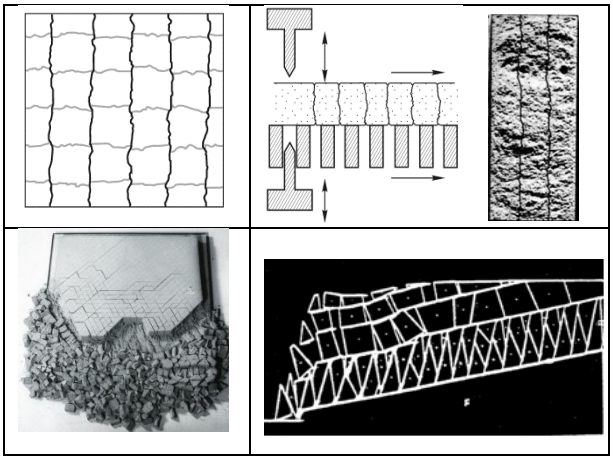

*Figure 2. A study in contrasts: physical modelling using tension-fracture generation, and numerical modelling using μDEC: this example demonstrates a friction angle for the joints of $\varphi = 20°$.*

*flexibility* of the two approaches is readily imagined from Figure 2. The single numerical slope model demonstrates the influence of changed friction angles, and was reported some years later, in Cundall et al., 1977 (1975 conference).

Despite the shortcomings of physical tension-fracture models, the writer nevertheless discovered that the peak shear strength of these rough and clearly unweathered tension fractures could be described by a simple relation involving the *uniaxial compression strength* ($\sigma_c$) of the model material (Barton, 1971). This was to prove useful.

$$\tau = \sigma_n \tan [20 \log (\sigma_c / \sigma_n) + 30°] \quad (1)$$

This equation, and simple links to peak dilation angle, proved to be the unweathered and roughest 'end-member' of the Barton and Choubey, 1977 equation for the peak

shear strength of rock joints, which followed some years after the testing of tension fractures.

$$\tau = \sigma_n \tan [ \text{JRC} \log (\text{JCS} / \sigma_n) + \varphi_r^o ] \qquad (2)$$

Here the *joint roughness coefficient* (JRC), the *joint wall compression strength* (JCS) and the *residual friction angle* ($\varphi_r$) can each assume lower magnitudes, caused by roughness JRC < 20, and variable weathering (JCS < $\sigma_c$, and $\varphi r < \varphi_b$. The first equation was based on *direct shear tests* of more than 200 artificial tension fracture samples, while the second equation was based on DST of 130 rock joint samples, some of them slightly weathered.

Physical models, each of 40,000 blocks, created for the rock slope stability studies by Barton, 1971, were followed some years later (Figure 4), by model studies of caverns for underground nuclear power plants, studying the generic effect of joint-set (fracture) orientation, anisotropy due to one dominant joint set, and horizontal stress variation in models with 20,000 blocks. This research was performed in NGI, Oslo. Barton and Hansteen, 1979 also compared the physical 'jointed' models with FEM continuum analyses.

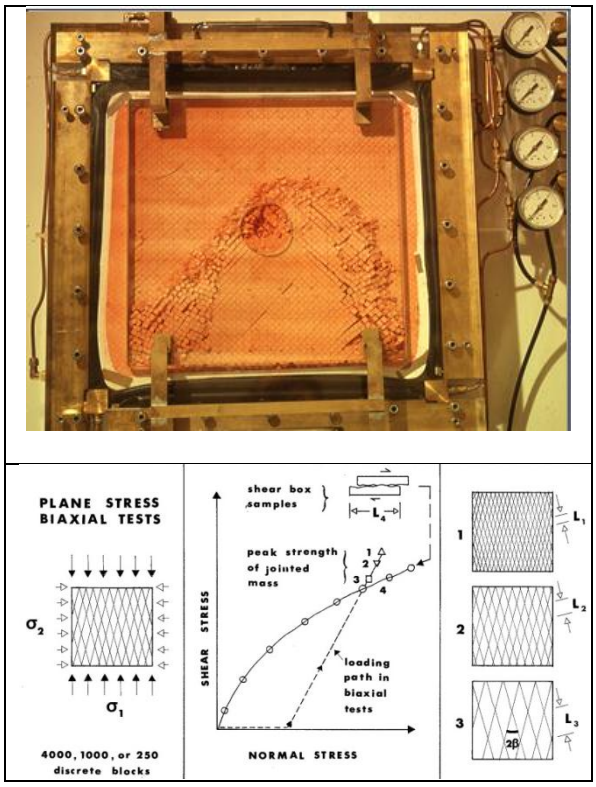


*Figure 3. Biaxially loaded two-dimensional physical models with respectively 250, 1000 or 4000 discrete blocks helped to give clues about scale effects caused by different block sizes. These physical models were described by Barton and Hansteen, 1979, therefore pre-dating UDEC-BB. It was noted that linear 'stress-strain' curves resulted when loading 4000-blocks models in biaxial shear. Convex curves were registered with larger block sizes.*

Some ten years later, this physical model experience was put to the test in the modelling of the planned Gjøvik cavern of 62 m span, using UDEC-BB. Figure 5 shows the input data, including BB parameters, the joint geometry from observations in surrounding caverns, and application of a high horizontal stress based on local stress measurements.

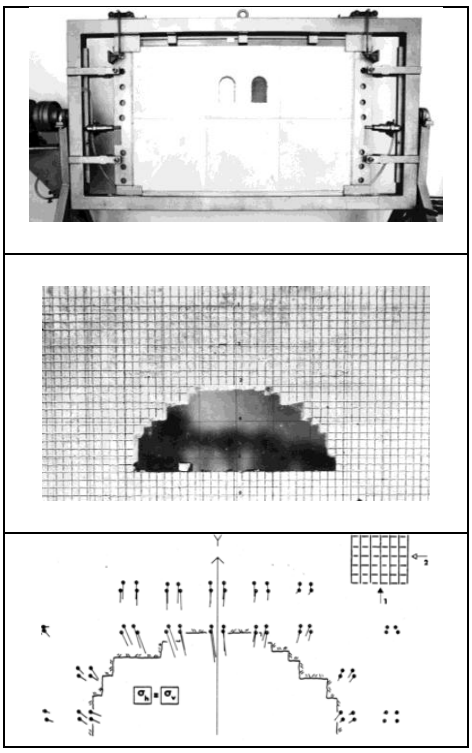

*Figure 4. Tension-fracture models consisting of 20,000 blocks, with three different joint patterns, and two different levels of applied horizontal stress, demonstrated that excavation of large caverns near the surface could cause upward (heave) or downward (subsidence) of the overlying 'rockmass'. Joint orientation effects and horizontal stress effects were coupled.*

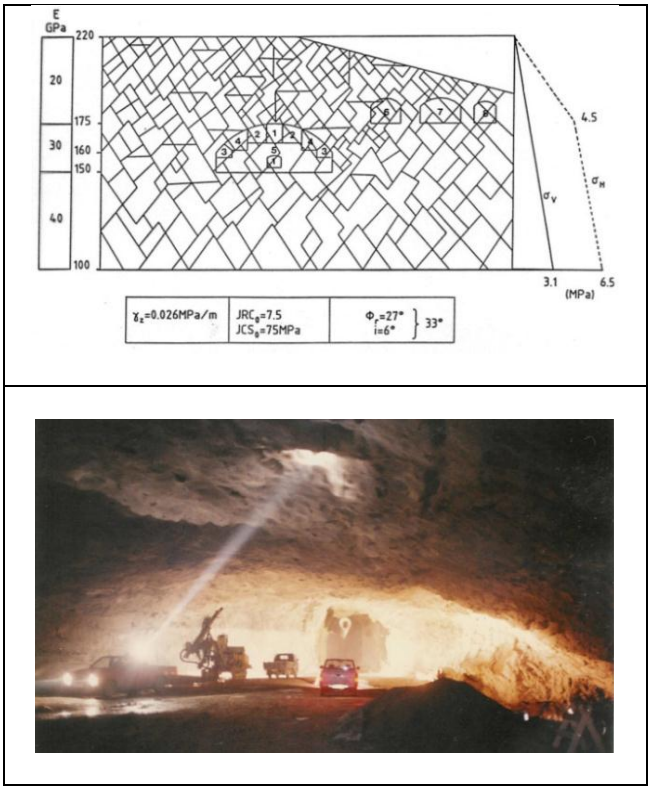


*Figure 5. The UDEC-BB model shown above, gave a good (Class A) prediction of 7 to 9 mm downward movement. (Barton et al., 1994). A view of the huge (stages 1 to 4) top-heading is shown.*

## 3. SHEAR FAILURE AROUND MODEL OPENINGS

Joint oil-industry borehole stability studies performed at NGI in the late eighties, provided consistent evidence of shear failure development in the form of log-spiral surfaces, with physically measured shear displacements. The model studies involved drilling into anisotropically loaded model sandstones in a 0.5 x 0.5 x 0.5 m polyaxial cell. Drilling could be performed in various directions in relation to the three independent principal stress directions, by drilling through pre-welded holes in the flatjacks.

*Figure 6. Log-spiral shearing with a 45º inclined hole drilled in the direction of $\sigma_H$ into a stressed block of model sandstone, with principal stress ratios $\sigma_v = 1$, $\sigma_H = 0.8$, $\sigma_h = 0.4$. Addis et al., 1990.*

The log-spiral form of failure has been seen when inspecting TBM headrace tunnels in massive sections of marble, and also in schists, where the estimated theoretical maximum tangential stress ($\sigma_\theta = 3\sigma_1 – \sigma_3$) was presumably exceeding the 'limit' of 0.4-0.5 x UCS, i.e. increased SRF in the Q-system. The onset of stress-slabbing and even rock bursting is seen if the ratio of UCS/$\sigma_\theta$ continues to rise with depth of cover exceeding 1 and even 2 km. Norwegian road tunnels have exceeded 1 km depth several times, but reached 1.4 km at the Lærdal Tunnel of 24.5 km length, with three caverns of 30 m span at almost this depth. Stress failure may be extensional when in hard dilatant rocks.

## 4. MODELLING FAILURE IN A ROCK MASS

The tunnel break-out that developed when excavating the Canadian URL mine-by experimental tunnel by line-drilling, was in response to obliquely acting, high and strongly anisotropic stresses. It is shown in Figure 7. The accompanying shortcomings of continuum modelling with *'c plus $\sigma_n$ tan $\varphi$'* shear strength assumptions, as partially illustrated in the same figure, should have alerted our profession for change already ten years ago.

Attempts to model 'break-out' phenomena such as those illustrated are not realistic with standard Mohr Coulomb or Hoek Brown failure criteria, because the *actual failure* mode is not following our long-standing expectation of *'c plus $\sigma_n$ tan $\varphi$'* for the strength of rock masses. In fact Müller indirectly pointed this out already in 1966.

The intact rock fails at small strain (in tension if hard and dilatant), in shear (if less dilatant), followed by the mobilization of friction along the new failure surfaces (if not ejected), followed by mobilization of surrounding joint surfaces. This of course is a complicated test of our present numerical modelling capabilities, and complex-algebra input data for 'c' and 'φ' as in Table 1, cannot by any stretch of the imagination, solve this challenging problem.

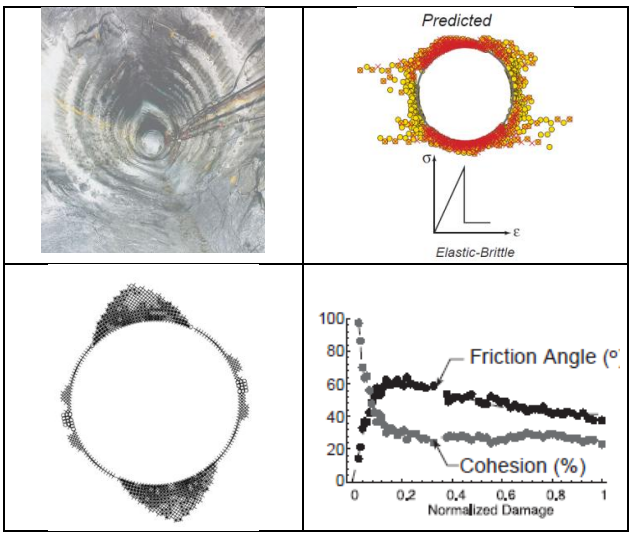


*Figure 7. An important demonstration of unsuccessful modelling by 'current methods', as given by Hajiabdolmajid et al., 2000. This is followed by their own more realistic degradation of cohesion and mobilization of friction, which was applied in FLAC.*

Rock masses actually follow an even more complex progression to failure, as suggested in Barton and Pandey, 2011, who recently demonstrated the application of a similar *'c then tan φ'* modelling approach, but applied it in FLAC 3D, for investigating the behaviour of multiple mine-stopes in India. A further break with convention was the application of peak 'c' and peak 'φ' *estimates* that were derived directly from mine-logged Q-parameters, using the CC and FC parameters suggested in Barton, 2002. For this method, an estimate of UCS is also required. CC (cohesive component) and FC (frictional component) are derived from separate 'halves' of the formula for $Q_c = Q \times \sigma_c / 100$.

*Table 1. The remarkable complexity of the algebra for estimating c' and φ' with Hoek-Brown based formulations (equations 4 and 6) are contrasted with the simplicity of equations 3 and 5, derived by 'splitting' the existing $Q_c$ formula into two parts, as described in Barton, 2002. ($Q_c = Q.\ \sigma_c/100$, with $\sigma_{ci}$ expressed in MPa).*

| | | |
|---|---|---|
| FC | $"\phi" \approx \tan^{-1}\left(\frac{J_r}{J_a} \times \frac{J_w}{1}\right)$ | (3) |
| | $\phi' = a\sin\left[\frac{6am_b\left(s + m_b\sigma'_{3n}\right)^{a-1}}{2(1+a)(2+a) + 6am_b\left(s + m_b\sigma'_{3n}\right)^{a-1}}\right]$ | (4) |
| CC | $"c" \approx \left(\frac{RQD}{J_n} \times \frac{1}{SRF} \times \frac{\sigma_c}{100}\right)$ | (5) |
| | $c' = \frac{\sigma_{ci}\left[(1+2a)s + (1-a)m_b\sigma'_{3n}\right]\left(s + m_b\sigma'_{3n}\right)^{a-1}}{(1+u)(2+a)\sqrt{1 + \left(6am_b\left(s + m_b\sigma'_{3n}\right)^{a-1}\right) / \left((1+a)(2+a)\right)}}$ | (6) |

It should be emphasised that all the Q-parameter ratings developed long ago by Barton et al. 1974, were successively improved by 6 months of trial-and-error fitting to required rock bolting needs (bolting is compensating for *low frictional strength*), and to required shotcreting needs (shotcrete is compensating for *low cohesive strength*). There is therefore *some case-record based support* for these parameters. $Q_c$ seems to be composed of 'c' x tan 'φ', not +.

*Table 2. Illustration of parameters CC (seems to be MPa ?) and FC° (friction angle), for a declining sequence of rock mass qualities, with simultaneously reducing $\sigma_c$ (MPa). $V_P \approx 3.5+\log Q_c$ (km/s), and $E_m \approx 10\ Q_c^{1/3}$ (GPa) were suggested in Barton, 2002.*

| RQD | Jn | Jr | Ja | Jw | SRF | Q | $\sigma_c$ | $Q_c$ | $FC^\circ$ | CC | $V_p$ | $E_m$ |
|---|---|---|---|---|---|---|---|---|---|---|---|---|
| 100 | 2 | 2 | 1 | 1 | 1 | 100 | 100 | 100 | 63 | 50 | 5.5 | 46 |
| 90 | 9 | 1 | 1 | 1 | 1 | 10 | 100 | 10 | 45 | 10 | 4.5 | 22 |
| 60 | 12 | 1.5 | 2 | 0.66 | 1 | 2.5 | 50 | 1.25 | 26 | 2.5 | 3.6 | 11 |
| 30 | 15 | 1 | 4 | 0.66 | 2.5 | 0.1 | 33 | 0.04 | 9 | 0.3 | 2.1 | 3.5 |

The pairs of parameters RQD/Jn and Jr/Ja are already being logged at a lot of tunnels and caverns, and also in mines, following Potvin and Matthews method, and the subsequent Modified Stability Graph, now in common use for preliminary stope dimensioning in many countries.

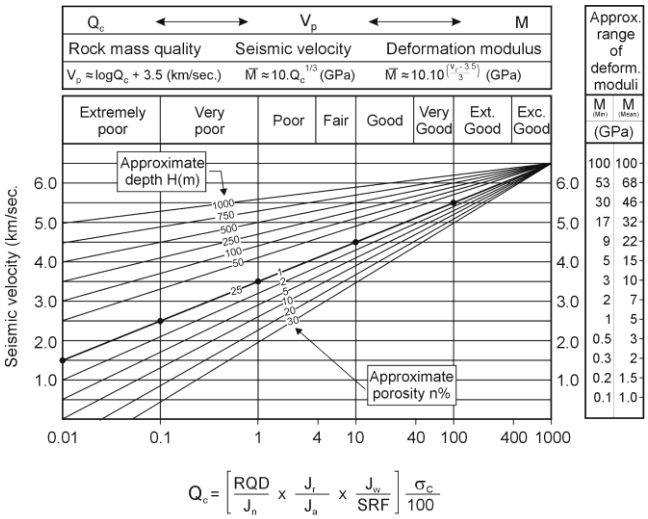


$$Q_c = \left[\frac{RQD}{J_n} \times \frac{J_r}{J_a} \times \frac{J_w}{SRF}\right] \frac{\sigma_c}{100}$$

*Figure 8.The integration of rock mass quality and seismic velocity, with adjustment (+ve) for depth (or stress level) and porosity (-ve), and rock strength. Estimates of static deformation modulus (right-hand column) should also be depth dependent. Barton, 1995.*

## 5. MODELLING A COMPACTING RESERVOIR

Seabed subsidence above the Ekofisk reservoir resulted in the raising of all platforms by 6 m, and provision of a 100 m diameter protective wall, and final re-location of operations away from the centre of the 9 x 14 km field. Since 1986 compaction has at least doubled, despite extensive sea-water injection for pressure maintenance that also caused inevitable weakening of the chalk.

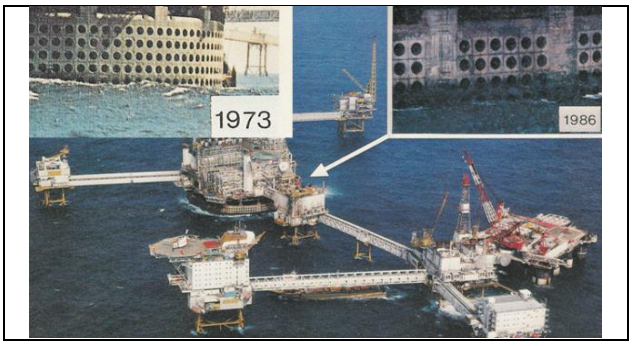


*Figure 9. A view of the Ekofisk reservoir in the North Sea, where compaction of the jointed-chalk reservoir of 300 m thickness at 3 km depth caused increasing sea-bed subsidence that amounted to about 4 m when investigations began in 1985-1987. Now it is 10m.*

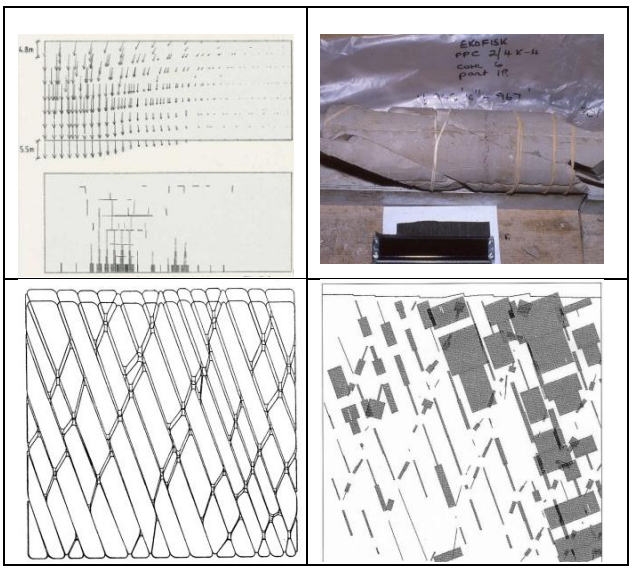

*Figure10. Top: Axi-symmetric UDEC-MC modelling of the ratio of subsidence/compaction (S/C) and two of the tested joint samples from Ekofisk. Bottom: UDEC-BB 'uniaxial-strain' M-H modelling of a vertical 1.5x1.5 m 2D-element of jointed Ekofisk chalk, which had a porosity of 40%. Input data was obtained from JRC and JCS characterization of numerous joint samples. Barton et al., 1986.*

The down-dip shearing that can occur despite one-dimensional strain, is a fundamental necessity for the continued conductivity of the dipping joints, as the matrix is of low permeability, and cannot otherwise be well drained.

During exploration, slickensided joints in the chalk *were not observed*. According to Philip's geologist (H. Farrell, pers. comm.), slickensiding *was observed* in some much later cored holes connected with the water-injection operations, after 1985. Production was causing joint shearing, and is presently a seemingly ignored part of 4D interpretation, by those focussing only on 'continuum based' phenomena in producing reservoirs. (Barton 2006).

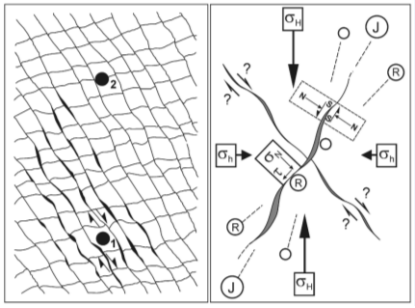

*Figure 11. A scenario (exaggerated here) involving maintenance of permeability through shearing and slight dilation is also consistent with analysis of deep-well conductors and non-conductors, and should be relevant to continued production from weak reservoir rocks. Note the possibility of by-passing fluid with incorrect interpretation, as also in numerous geothermal projects.*

## SHEAR STRENGTH AT EXTREME STRESS LEVELS

In 1976 the author proposed a 'critical state' concept for the shear strength of intact rock at high stress, which involved both the expectation and the actual *horizontal orientation* of the Mohr strength envelope. Recently, this

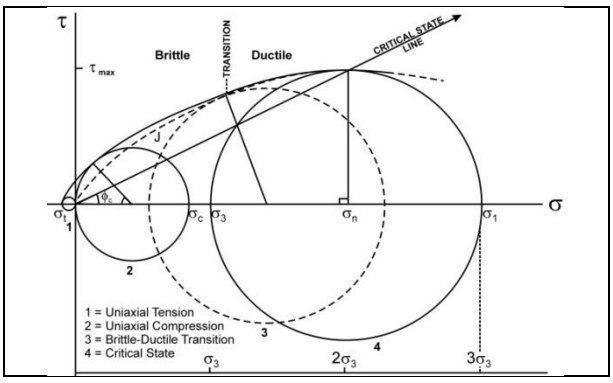


*Figure 12. Critical state line for intact rock at extreme stress levels (Barton, 1976), suggested the limiting condition $\sigma_1 = 3\sigma_3$. Singh et al., 2011 show that most often, the critical value of $\sigma_3 \approx \sigma_c$. This seems to be logical, and helps to define a strength-envelope curvature which correctly matches test data at all confining pressure levels, and improves upon all existing strength criteria.*

concept has been applied to better define the curvature of intact rock strength envelopes. A few tests at low confining pressures provide all the data needed for extrapolation to high levels of confinement. The elegant Singh et al., 2011 shear strength criterion heralds a new era in rock mechanics understanding.

Since a blend of theory and empiricism has been promised in the title, with possible application to problem solving in rock engineering, the final figure to be presented will be of the tilt testing concept. This is at the other end of an extreme stress range, and has been widely applied.

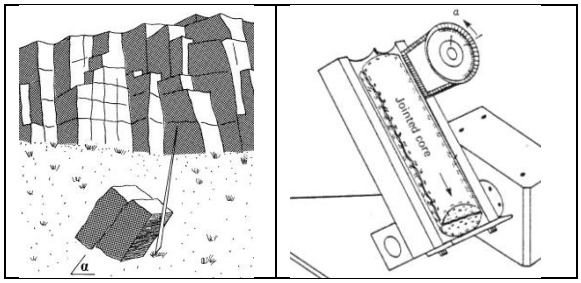


*Figure 13. The tilt test result can be extrapolated from 0.001 to 10 MPa, and can be performed on samples of 10 cm to 1 m in size. The same method has also been used on 5m long as-built rockfills.*

## CONCLUSIONS

Those who restrict their rock mechanics experience to GSI-based isotropic continuum modeling, inevitably miss many exciting insights in the rewarding field of rock engineering, which is mostly executed in jointed, anisotropic water-bearing rock-masses, which usually vary from location to location. Complex algebra and multiple decimal places are irrelevant in such a variable medium.

## REFERENCES


Addis, M.A., Barton, N., Bandis, S.C. & Henry, J.P. 1990. Laboratory studies on the stability of vertical and deviated boreholes. *65th Ann. Tech. Conf. & Exhibition of the Society of Petroleum Engineers*, New Orleans.

Bandis, S., Lumsden, A. & Barton, N. 1981. Experimental studies of scale effects on the shear behaviour of rock joints. *Int. J. Rock Mech. & Min. Sci.* 18, 1-21.

Bandis, S., Lumsden, A.C. & Barton, N. 1983. Fundamentals of rock joint deformation. *Int. J. Rock Mech. & Min. Sci.* 20: 6: 249-268.

Barton, N. 1971. *A model study of the behaviour of steep excavated rock slopes. Ph.D. Thesis*, Univ. of London.

Barton, N. 1976. The shear strength of rock and rock joints. *Int. Jour. Rock Mech. Min. Sci.* 13, 9: 255-279.

Barton, N. & Choubey, V. 1977. The shear strength of rock joints in theory and practice. *Rock Mechanics*, Vienna: Springer; 1/2:1-54.

Barton, N. & Hansteen, H. 1979. Very large span openings at shallow depth: Deformation magnitudes from jointed models and F.E. analysis," *4th Rapid Excavation and Tunnelling Conference, RETC*; Atlanta Georgia, Vol. 2: 1131-1353. A.C. Maevis and W.A. Hustrulid (Eds), *American Inst. of Min. & Metall, & Petroleum Engineers*, Inc. New York, New York, 1979.

Barton, N. 1986. Deformation phenomena in jointed rock. 8th Laurits Bjerrum Memorial Lecture, Oslo. *Geotechnique*, Vol. 36: 2: 147-167.

Barton, N., Hårvik, L., Christiansson, M., Bandis, S., Makurat, A., Chryssanthakis, P. & Vik, G. 1986. Rock mechanics modelling of the Ekofisk reservoir subsidence. *Proc. 27th US Rock Mech. Symp*., Univ. of Alabama.

Barton, N., By, T.L., Chryssanthakis, P., Tunbridge, L., Kristiansen, J., Løset, F., Bhasin, R.K., Westerdahl, H. & Vik, G. 1994. Predicted and measured performance of the 62m span Norwegian Olympic Ice Hockey Cavern at Gjøvik. Int. J. Rock Mech, Min. Sci. & Geomech. Abstr. 31:6: 617-641. Pergamon.

Barton, N. 1995. The influence of joint properties in modelling jointed rock masses. Keynote, *8th ISRM Congress*, Tokyo, 3: 1023-1032, Balkema, Rotterdam.

Barton, N. 2002. Some new Q-value correlations to assist in site characterization and tunnel design. *Int. J. Rock Mech. & Min. Sci*., 39: 185-216.

Barton, N. 2006. *Rock Quality, Seismic Velocity, Attenuation and Anisotropy.* Taylor & Francis, UK & Netherlands, 729 p.

Barton, N. and S.K.Pandey, 2011. Numerical modelling of two stoping methods in two Indian mines using degradation of c and mobilization of φ based on Q-parameters. *Int. J. Rock Mech & Min.Sci.48,7, 1095-1112.*

Cundall, P.A., Voegele, M.D. and Fairhurst, C. 1977. Computerized design of rock slopes using interactive graphics for the input and output of geometrical data. *Proc. of 16th US Symp. on Rock Mechanics*, Minnesota 1975, Vol.1, 5-14, C. Fairhurst and S.L. Crouch (Eds). American Soc. of Civil Engineers, New York.

Hajiabdolmajid,V., C. D. Martin and P. K. Kaiser,. Modelling brittle failure. *Proc. 4th North American Rock Mechanics Symposium, NARMS 2000* Seattle J. Girard, et al., (Eds), 991–998. A.A. Balkema, Rotterdam.

Müller, L. 1966. The progressive failure in jointed media. *Proc. of ISRM Cong*., Lisbon, 3.74, 679-686.

Singh, M., A. Raj & B. Singh, 2011. Modified Mohr-Coulomb Criterion for Non-linear Triaxial and Polyaxial Strength of Intact Rocks. *Int. J. Rock Mech. & Min. Sci.* Vol. 48, Issue 4, 546-555.